Observation of Doppler-free electromagnetically induced transparency in atoms selected optically with specific velocity

Hoon Yu, Kwan Su Kim, Jung Dong Kim, Hyun Kyung Lee, and Jung Bog Kim*
Department of Physics Education, Korea National University of Education, Chung-Buk 363-791, Korea
(Received 3 July 2011; published 18 November 2011)

We observed an electromagnetically induced transparency signal in a four-level system with optically selected rubidium atoms at specific velocities in a room-temperature vaporized cell. Since the atoms behave like cold atoms in the selected atomic view, the observed signals coincide with a trapped atomic system. According to this result, we can observe Doppler-free signals, which correspond from 1.2 to 1.0 K in a Doppler-broadened medium. And the selected atoms have velocity components of $\pm(131 \pm 3)$ MHz per wave number. Our experimental results can provide insight for research in cold media.

DOI: 10.1103/PhysRevA.84.052511 PACS number(s): 32.10.Fn, 32.80.Qk, 32.80.Xx, 32.80.Wr

I. INTRODUCTION

Coherent effects based on atomic energy levels have attracted considerable attention in recent years. Coherent population trapping (CPT) [1,2], electromagnetically induced transparency (EIT) [3–9], and lasing without inversion occur by coherent interaction of atoms and laser beams. In a three-level system, λ-type EIT, which can be observed when two ground states are coherently coupled by two resonant coherent fields where the excited state is common, is a representative phenomenon. In this case, a weak probe laser field is seldom absorbed even on resonance. Since EIT provides a narrower spectral width than the natural linewidth, the atomic medium turns out to be very highly normal dispersive. Many studies have been carried out using EIT in applications, such as slow light, light storage, optical switching, quantum information processing, magnetometry, and atomic frequency references [3–14]. EIT signals also can be observed in various other energy-level schemes, namely, the so-called ladder, *V*-, *Y*-, or *N*-type systems [5–7,15–20].

As with rising laser-cooling technologies, which are used to enhance nonlinear effects by increasing the number of interacting atoms, EIT also has been reported in magneto-optically trapped or even coherent atomic media, such as a Bose-Einstein condensate [21–23]. Despite many outstanding achievements with cold atoms, there are some difficulties in preparing such cold media. If the observation of coherent effects, such as cold atoms in thermal atoms, is feasible, these results can provide experimental information to anticipate and to design an experimental scheme.

Many studies reported recording Doppler-free spectra in Doppler media by using counterpropagation of both the pump beam and the probe beam since saturated spectroscopy was reported [24,25]. Variation in the population of atomic states by using two counterpropagating laser beams, known as optical pumping, can be observed when two beams seem to be resonant with the atomic transition in the atomic frame. Therefore, this technique is used to observe the Doppler-free spectrum. For example, velocity-selective absorption (VSA) is related to an atomic group having a specific velocity component in the direction of the beam's propagation. Since only specific velocity components involving zero interact resonantly with laser fields, optical pumping can be used to observe a Doppler-free spectrum in a Doppler-broadened medium. Appropriately using this experimental technique, it is possible to observe coherent effects, such as a cold-atom medium in a thermal atom medium. In this paper, we describe experimental results in the atomic vapor cell at room temperature, which are very similar to EIT signals obtained in cold atoms.

II. EXPERIMENTAL SETUP

The experimental setup is shown in Fig. 1. We use three independent external cavity diode lasers with no phase matching. Their linewidths are less then 1 MHz; however, they will become a little broader because of frequency modulation for locking the laser frequency to the atomic transition line. Co-propagating pumping and coupling beams are overlapped by about 1° with the probe beam, which counterpropagates in the Rb vapor cell, which is 5-cm long and 2.54 cm in diameter without coating for antirelaxation. All laser fields are linearly polarized where the probe field is perpendicular to coupling and pumping fields have the same polarization. Coupling and pumping beams are overlapped by a nonpolarized beam splitter [(BS) in Fig. 1] and pass through a 3.2-mm aperture, while the probe beam passes through a 0.9-mm aperture. The power of each beam is controlled by a combination of polarization BSs and HWPs. The air-conditioned room temperature is maintained at 293 K. We compensate the terrestrial magnetic field by shielding the perimeter of the cell with mu metal.

We consider the six-level hyperfine states of a ^{87}Rb D_2 transition in Fig. 2. For ^{87}Rb, the splitting of lower levels ($5S_{1/2}$, $F = 1,2$) is 6834 MHz, while the upper levels ($5P_{3/2}$, $F' = 0$–3) are split by 71, 157, and 267 MHz, respectively. In this paper, the resonant transition frequencies between the hyperfine ground state ($F = 1,2$) and the excited state ($F' = 0$–3) are denoted by $\omega_{\mathrm{FF'}}$. Here, ω_{b}, ω_{c}, and ω_{p} represent the frequencies of the probe, coupling, and pumping beams, respectively. Detuning of each laser beam from ω_{12} is represented as Δ_{b}, Δ_{c}, and Δ_{p}, respectively.

Figure 2 shows predictable configurations of the experimental condition when ω_{b} and ω_{c} are locked on the crossover between ω_{23} and ω_{22} of ^{87}Rb atoms, while the pumping (ω_{p})

*jbkim@knue.ac.kr

 ©2011 American Physical Society

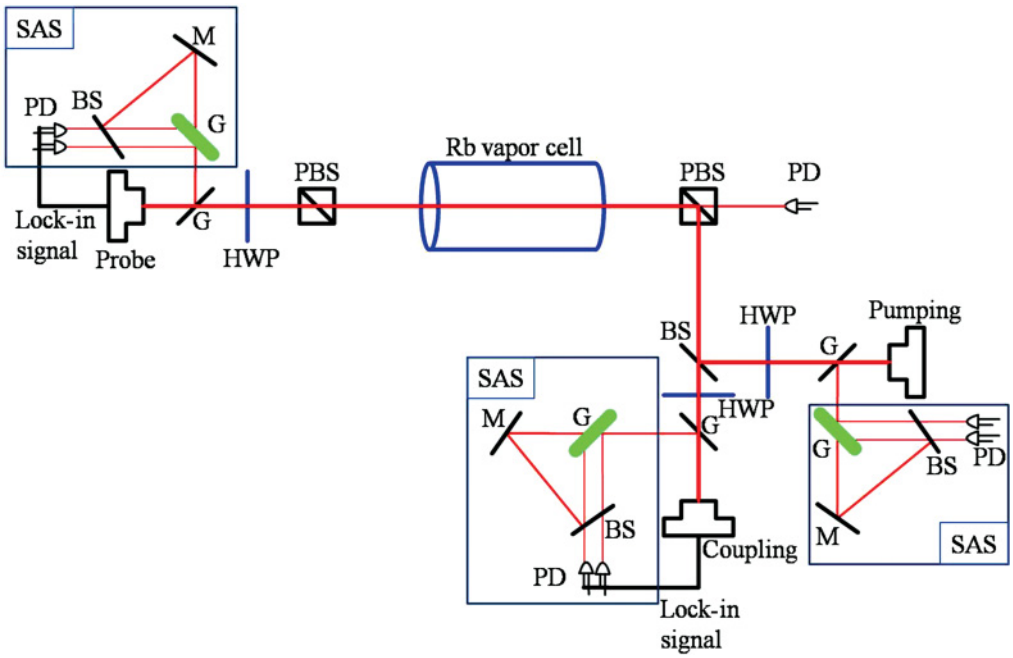

FIG. 1. (Color online) Experimentalsetup for observing Doppler-free EIT spectra in a vapor cell [PD, photodiode; (HWP), half-wave plate; BS; G, glass; (SAS), saturated absorption spectroscopy]. SAS in each laser system is used for frequency calibration of the obtained spectrum or to obtain an error signal for frequency stabilization.

beam is swept over the range of the $5S_{1/2}(F = 1) \rightarrow 5P_{3/2}$ (all hyperfine states, $F' = 0$–2). The solid lines represent the frequency of each laser beam at the atomic frames when $\omega_p \pm \vec{k_p} \cdot \vec{v}_{\text{atom}}$ satisfies the resonance condition. The dashed lines represent the laboratory frame. The (a)–(e) cases in Fig. 2 represent energy-level schemes comprising two laser beams ω_b and ω_p. And each (f)–(j) case represents a scheme adding the coupling beam (ω_c) on (a)–(e), respectively. We let the direction of the probe-beam propagation be the positive direction of atomic motion.

III. EXPERIMENTAL RESULTS

The main idea of observing Doppler-free EIT signals in a Doppler-broadened medium is based on optical pumping to another hyperfine ground state. When the pumping beam of 6.6 mW/cm^2 and the probe beam of 35 μW/cm^2 counterpropagate through a thermal atomic medium, a VSA spectrum (VSAS) due to optical pumping can be observed. The upper signal in Fig. 3 shows a typical VSAS where the probe frequency is stabilized on the crossover that occurs at the center frequency of the ω_{23} and ω_{22} transition lines of the ^{87}Rb atoms while the pumping beam's detuning is swept. The lower signal in Fig. 3 is a saturated spectrum of the pumping beam, which is used for the reference frequency.

Each VSAS in Fig. 3 occurs due to each corresponding energy-level schematic shown in Fig. 2, respectively. The coupling laser field is not used in Fig. 3 only for VSAS. Although there are six structures, only four structures are observed. For example, the c dip in Fig. 3 can be observed when Δ_p is $-(132 \pm 2)$ MHz at the laboratory frame. The nonlinear scanning of the pumping laser causes the uncertainty of Δ_p. In other words, when the frequency of the pumping beam is calibrated with distance ω_{12} and X_{12} as a standard, Δ_p is -134 MHz in the c case. In the other standard $\omega_{12} \sim \omega_{10}$, Δ_p is calculated to be -130 MHz. However, these frequency detunings become $\Delta_b = \Delta_p = 0$ MHz in the moving frame of the atoms that have a (132 ± 2) MHz/WN (wave number) velocity component along the direction of the probe-beam propagation. Therefore, the condition for VSAS can be satisfied. A MHz/WN unit is used to represent atomic speed in terms of megahertz per wave number of the laser beam.

Each d and e case in Fig. 3 is observed when each Δ_p is $-(24 \pm 2)$ and (132 ± 2) MHz, which corresponds to the specific velocity components $-(103 \pm 2)$ and $-(103 \pm 2)$ m/s in *Système International* units, respectively. In the (e) case in Fig. 2, atoms that have a (132 ± 2) MHz/WN velocity component do not contribute to the signal due to the selection rule, forbidden transition $F = 1 \rightarrow F' = 3$, but atoms of the $-(132 \pm 2)$ MHz/WN velocity component do. Especially in the (b) case, two groups of atoms contribute to the absorption dip. In the first group of atoms with the (132 ± 2) MHz/WN velocity component, the probe frequency is resonant on ω_{22}, and the pumping frequency is resonant on ω_{11} in the left part of Fig. 2(b). In the second group of the (296 ± 5) MHz/WN velocity component, the probe and the pumping beams are resonant at ω_{21} and ω_{12}, which is shown in the right part of Fig. 2(b). Although another VSAS can be observed at $\Delta_p = -448$ MHz as (a) in Fig. 2, we could not observe the signal because it may have been too weak.

The linewidths of dips from (b) to (e) are 32, 32, 29, and 31 MHz, which correspond to Doppler linewidths of 1.2 – 1.0 K. These temperature ranges can be calculated into the velocity components of $\pm 10.7 \sim 9.8$ m/s. Although our VSAS has cold-atom-like effects, it shows more broadened spectra

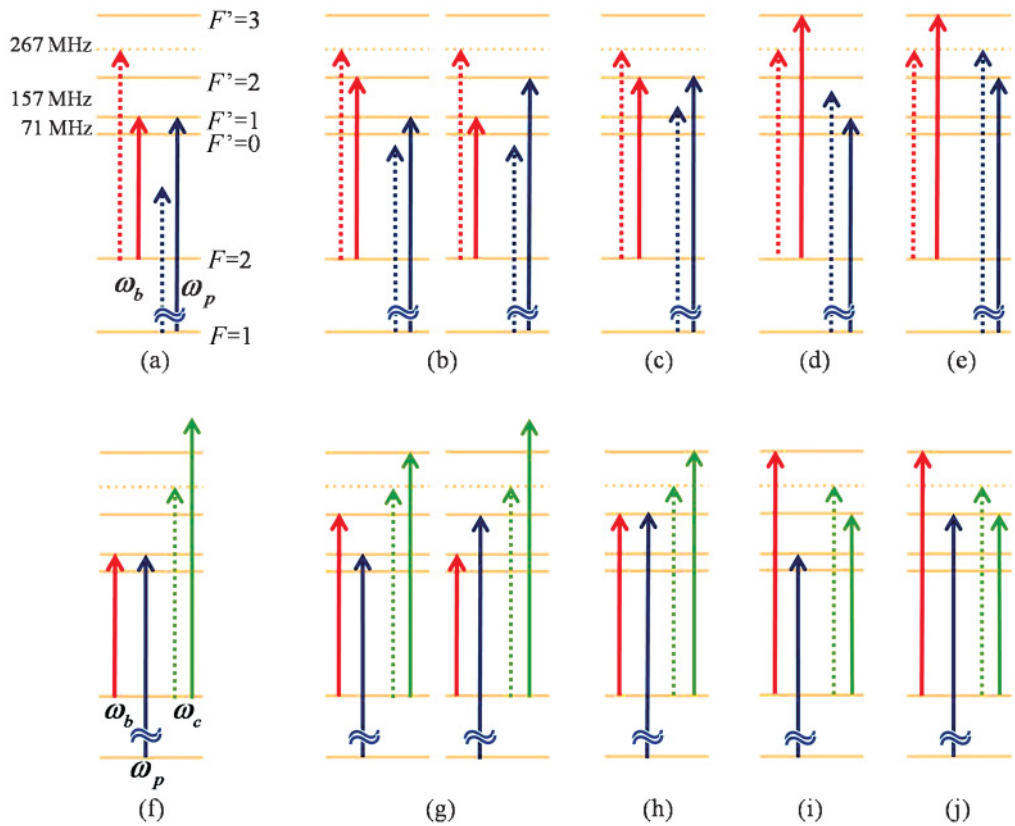

FIG. 2. (Color online) Schemesof the ^{87}Rb atomic system. The solid lines represent laser frequencies in the atomic frame. The dashed lines indicate the laboratory frame. The (a)–(e) cases represent schemes comprising both probe (ω_b) and pumping (ω_p) beams. And each (f) – (j) case represents a scheme adding the coupling beam (ω_c) on (a)–(e), respectively. Each experimental spectrum of an (a)–(e) scheme appears in Fig. 3, and each experimental spectrum of an (f)–(j) scheme appears in Fig. 4. Δ_p is (a) −448 MHz, (b) −291 MHz, (c) −134 MHz, (d) −23 MHz, (e) 134 MHz, (f) −448 MHz, (g) −291 MHz, (h) −134 MHz, (i) −23 MHz, and (j) 134 MHz in the laboratory frame. The velocity component consisting in each atomic frame is (a) 291 MHz/WN, (b) 134 MHz/WN and 291 MHz/WN, (c) 134MHz/WN, (d) −134 MHz/WN, (e) −134 MHz/WN, (f) 291 MHz/WN, (g) 134 MHz/WN and 291 MHz/WN, (h) 134MHz/WN, (i) −134 MHz/WN, and (j) −134 MHz/WN.

than the cold atoms. In our result, a small angle of about 1° between the probe and the pumping beam is allowed for easy separation to detect only the probe field. This induces Doppler broadening, which is the main reason for the broadening as well as the natural linewidth, although the transit time, power of the laser beam, and collisions with other atoms and cell walls are reasons for negligible broadening. The power broadening, which relates a strong pumping beam ($5S_{1/2}F = 1 \rightarrow 5P_{3/2}F' = 2$), 6.6 mW/cm^2, is approximately 10 MHz. And the transit-time-broadening-related limited beam size, 0.9 and 1.6 mm on the waist of the probe and pumping beams, respectively, is less than 1 MHz at room temperature.

As in both (a) and (c) cases, even though two laser beams satisfy the condition for a Λ-type EIT scheme in the atomic frame, EIT signals are not observed because there is not enough pumping intensity.

By adding another beam called the coupling beam as represented by ω_c in Fig. 2, *N*-type EIT configurations, (h) and (j) cases in Fig. 2, appear at the moving atomic frame, despite the fact that all laser beams are nonresonant in the laboratory frame. From these schemes, we are able to observe the Doppler-free EIT spectrum as shown in Fig. 4. Even though some papers on thermal atoms report the effect of *V*-type EIT on the saturated spectrum [17], velocity-selective optical pumping effects in Λ-type systems [26], and Doppler-free electromagnetically induced absorption [27], our observation of Doppler-free *N*-type EIT signals with thermal atoms is a different phenomenon.

Figure 4 shows the nonlinear effect of a three-photon process where $I_b = 35\ \mu$W/cm^2, $I_p = 6.6$ mW/cm^2 or 7.4 mW/cm^2, and $I_c = 135$ mW/cm^2. The signals g–j occur at $\Delta_p = -294, -134, -23$, and 134 MHz. In the g case shown in Fig. 4, two effects are overlapped. One is a *V*-type EIT related to the first group shown in the left part of Fig. 2(b), and the other is a VSAS related to the second group shown in the right part of Fig. 2(b). Therefore, the g dip due to two effects seems so flat. In the h case shown in Fig. 4, $\omega_b = \omega_{22}$, $\omega_p = \omega_{12}$, and $\omega_c = \omega_{23}$ at the 134 MHz/WN atomic frame. In the j case, $\omega_b = \omega_{23}$, $\omega_p = \omega_{12}$, and $\omega_c = \omega_{22}$ at the −134 MHz/WN atomic frame. These energy level schemes are described in Fig. 2. These h and j signals are *N*-type EITs. The relative transparency rate defined by the ratio "trans."/"abs." in Fig. 4 is 0.3 for both the h and the j cases with 6.6 mW/cm^2 of the pumping beam. The EIT signal in the h case disappears when the intensity of the pumping beam increases slightly to 7.4 mW/cm^2, although it barely changes

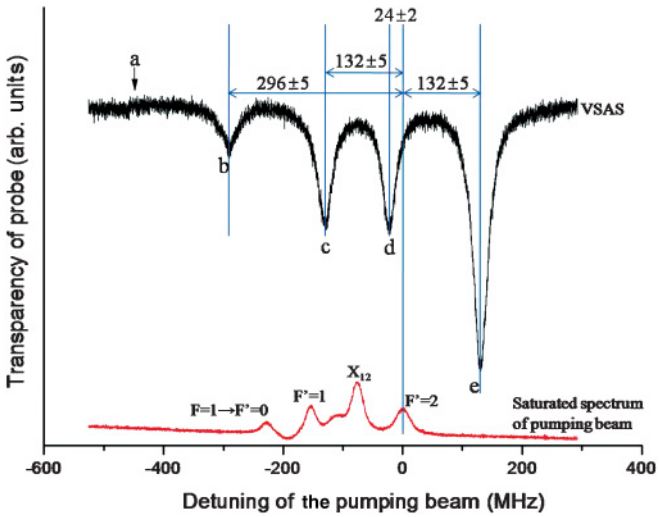

FIG. 3. (Color online) VSAS obtained by detection of the probe beam's transparency rate as Δ_p when ω_b is locked on the crossover between ω_{23} and ω_{22} of the ^{87}Rb atom. The upper signal is a VSAS. The lower signal shows a saturated spectrum of the pumping beam for the frequency standard. Note that b–e appear at $\Delta_p = -296 \pm 5$, -132 ± 5, -24 ± 2, and 132 ± 5 MHz.

in the j case. The range of pumping intensity for observing h EIT is narrow. Thus, the EIT signal for the h case is more sensitive to pumping power than the j case. The i case should show a *V*-type EIT spectrum with an incoherent pumping beam. However, we cannot find any transparent signal. We see very small absorption at the i position, which means that the probe beam interacts with a small number of atoms. We think this is because the optical pumping effect of the coupling beam is stronger than the optical pumping of the pumping

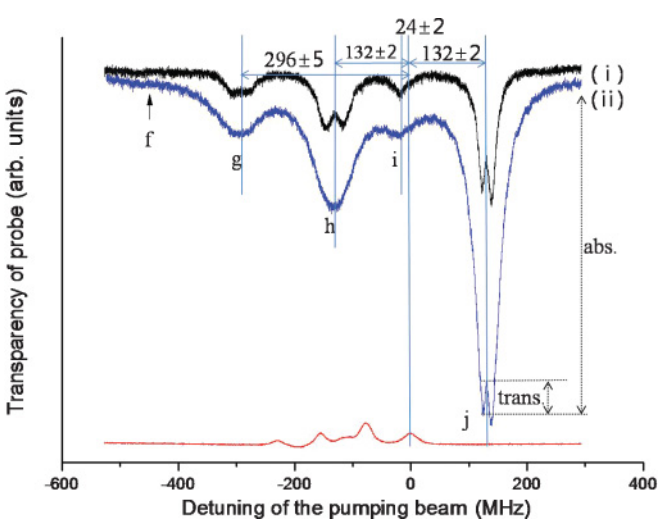

FIG. 4. (Color online) Doppler-free *N*-type EIT signals obtained by the detection of the probe-beam transparency rate as Δ_p when ω_b and ω_p are stabilized on the crossover between ω_{23} and ω_{22} of the ^{87}Rb atom with thermal atoms. The intensity of using each laser beam is $I_b = 35\ \mu\text{W/cm}^2$ and $I_c = 135\ \text{mW/cm}^2$. (i) $I_p = 6.6\ \text{mW/cm}^2$ and (ii) $I_p = 7.4\ \text{mW/cm}^2$. All laser frequencies in the atomic frame are presented in Fig. 2, and units are in megahertz.

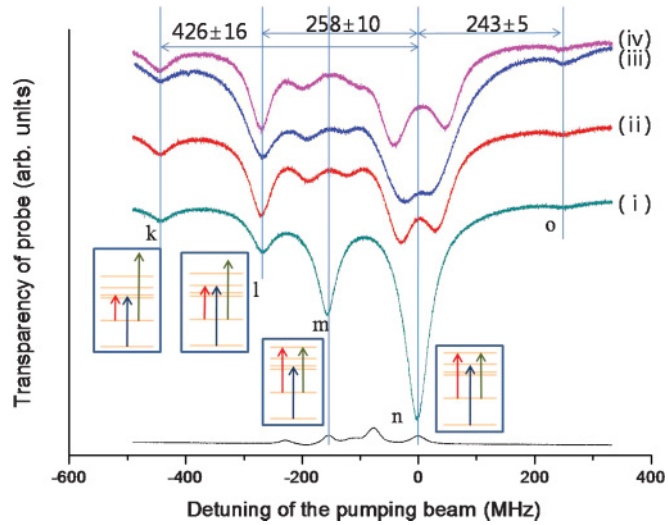

FIG. 5. (Color online) Probe-beamspectrum as Δ_p when ω_b and ω_c are resonant at ω_{23}. In all spectra, $I_b = 35\ \mu\text{W/cm}^2$. (i) $I_p = 3.4\ \text{mW/cm}^2$ and $I_c = 0\ \text{mW/cm}^2$, (ii) $I_p = 3.4\ \text{mW/cm}^2$ and $I_c = 299\ \text{mW/cm}^2$, (iii) $I_p = 11.8\ \text{mW/cm}^2$ and $I_c = 299\ \text{mW/cm}^2$, and (iv) $I_p = 3.4\ \text{mW/cm}^2$ and $I_c = 535\ \text{mW/cm}^2$.

beam, which does not provide the system with enough atoms. From these observations, we may conclude that laser intensities are strong parameters for *N*-type EIT in four-level systems.

Experimental and theoretical results related to EIT in four-level systems have been reported in previous studies [19–22]. For example, the j configuration in Fig. 4 generally has been realized for *N*-type EITs also with cold atoms [21,22]. The linewidth of the j signal corresponds to a 1.1-K Doppler temperature width due to the thermal motion of atoms, that is, atom-wall collisions, which means lower coherent interaction of trans. and abs. than that with cold atoms. Despite some differences, our results experimentally can provide insight into research in cold media, such as the coherent effect in multilevels and multiwave mixing.

When probe and coupling beams are locked on resonance ω_{23} in the laboratory, the velocity class with a $v = 0$ frame, VSAS, and Rabi splitting appears around the resonance transitions as shown in Fig. 5, which shows the spectrum of the probe beam as a function of Δ_p [28]. Of course, moving atoms should see laser fields with some detunings. Velocity components of 426 ± 16, 258 ± 10, 0, and 0 MHz/WN make corresponding k–o signals, respectively, as shown in Fig. 5(i) with counterpropagating probe and pumping beams. Greater uncertainty is induced with a large scan range. In the atomic frame, the k case in Fig. 5 corresponds to $\omega_b = \omega_{21}$, $\omega_c = \omega_{23} + (426 \pm 16)$ MHz and $\omega_p = \omega_{12}$. The l case occurs under the conditions of $\omega_b = \omega_{22}$, $\omega_c = \omega_{23} + (258 \pm 10)$ MHz, and $\omega_p = \omega_{12}$ in the atomic frame. The m and n cases occur in 0 MHz/WN atoms, which means that detunings in the laboratory frame are the same as those in the atomic frame. Thus, $\omega_b = \omega_{23}$, $\omega_c = \omega_{23}$, and $\omega_p = \omega_{11}$ at m, and $\omega_b = \omega_{23}$, $\omega_c = \omega_{23}$, and $\omega_p = \omega_{12}$ at n. In Figs. 5(ii)–5(iv), m and n show double dips due to Rabi-splitting effects of the resonant coupling beam. Under strong pumping intensities, an uninterpretable signal appears as in the o case in Fig. 5(iii).

IV. CONCLUSION

We were able to observe Doppler-free EIT signals and VSAS in a Doppler-broadened medium by using three laser fields. We interpreted each absorption dip as Δ_p with atomic energy-level schemes at the atomic frame. Even with the experimentally easy atomic vapor cell, velocity-selective Doppler-free EIT signals were directly compared with results that can be obtained in trapped atoms. The corresponding temperature of our Doppler-free signals was (1.1 ± 0.1) K, (31 ± 2)-MHz linewidth. This effective atomic temperature of velocity-selected atoms is a little higher than that for real cold atoms because moving atoms show a Doppler effect for the small angle of laser beams. In other words, velocity-selected atoms seem to be stopped, however, the spectrum obtained from the vapor cell shows the dependence on the angle between laser beams. Although CPT and EIT resonances have sub-Doppler linewidths, these resonances appear with linear absorption. Thus, CPT and EIT resonances in the vapor cell are within the very broad background absorption signal of about a 500-MHz linewidth. This broadened background is the limit compared with real cold atoms that have a few 10-MHz linewidths. Since our signal has no such broad background, despite a very small broadened background, our Doppler-free EIT signals experimentally can provide insight for research in cold media due to the narrow background absorption signal.

ACKNOWLEDGMENTS

This research was supported by the Basic Science Research Program through the National Research Foundation of Korea (NRF) funded by the Ministry of Education, Science and Technology (Grant No. 2010-0004145).

[1] G. Alzetta *et al.*, Nuovo Cimento B **36**, 5 (1976).
[2] G. Alzetta, L. Moi, and G. Orriols, Nuovo Cimento B **52**, 209 (1979).
[3] K. J. Boller, A. Imamoglu, and S. E. Harris, Phys. Rev. Lett. **66**, 2593 (1991).
[4] S. E. Harris, J. E. Field, and A. Kasapi, Phys. Rev. A **46**, R29 (1992).
[5] D. J. Fulton, S. Shepherd, R. R. Moseley, B. D. Sinclair, and M. H. Dunn, Phys. Rev. A **52**, 2302 (1995).
[6] M. Xiao, Y. Q. Li, S. Z. Jin, and J. Gea-Banacloche, Phys. Rev. Lett. **74**, 666 (1995).
[7] Y. Q. Li, S. Z. Jin, and M. Xiao, Phys. Rev. A **51**, 1754 (1995).
[8] R. R. Moseley, S. Shepherd, D. J. Fulton, B. D. Sinclair, and M. H. Dunn, Phys. Rev. Lett. **74**, 670 (1995).
[9] S. A. Hopkins, E. Usadi, H. X. Chen, and A. V. Durrant, Opt. Commun. **138**, 185 (1997).
[10] H. S. Moon, S. E. Park, Y. H. Park, L. Lee, and J. B. Kim, J. Opt. Soc. Am. B **23**, 2393 (2006).
[11] A. Kuzmich, W. P. Bowen, A. D. Boozer, A. Boca, C. W. Chou, L.-M. Duan, and H. J. Kimble, Nature (London) **423**, 731 (2003).
[12] M. D. Lukin and A. Imamoglu, Nature (London) **413**, 273 (2001).
[13] L. V. Hau, S. E. Harris, Z. Dutton, and C. H. Behroozi, Nature (London) **397**, 594 (1999).
[14] D. F. Phillips, A. Fleischhauer, A. Mair, R. L. Walsworth, and M. D. Lukin, Phys. Rev. Lett. **86**, 783 (2001).
[15] J. Gea-Banacloche, Y. Q. Li, S. Z. Jin, and M. Xiao, Phys. Rev. A **51**, 576 (1995).
[16] Y. Q. Li, S. Z. Jin, and M. Xiao, Phys. Rev. A **51**, R1754 (1995).
[17] Y. Wang, G. Xu, C. Ye, J. Zhao, S. Zhou, and Y. Liu, Phys. Rev. A **53**, 1160 (1996).
[18] J. Zhao, L. Wang, L. Xiao, Y. Zhao, W. Yin, and S. Jia, Opt. Comm. **206**, 341 (2002).
[19] C. Goren, A. D. Wilson-Gordon, M. Rosenbluh, and H. Friedmann, Phys. Rev. A **69**, 053818 (2004).
[20] G. S. Agarwal and W. Harshawardhan, Phys. Rev. Lett. **77**, 1039 (1996).
[21] H. Kang and Y. Zhu, Phys. Rev. Lett. **91**, 093601 (2003).
[22] H. Kang, L. Wen, and Y. Zhu, Phys. Rev. A **68**, 063806 (2003).
[23] S. E. Harris and L. V. Hau, Phys. Rev. Lett. **82**, 4611 (1999).
[24] T. W. Hänsch, I. S. Shahin, and A. L. Schawlow, Phys. Rev. Lett. **27**, 707 (1971).
[25] J. Duan, X. Qi, X. Zhou, and X. Chen, Opt. Lett. **36**, 561 (2011).
[26] S. Chakrabarti, A. Pradhan, B. Ray, and P. Ghosh, J. Phys. B **38**, 4321 (2005).
[27] M. G. Bason, A. K. Mohapatra, K. J. Weatherill, and C. S. Adams, J. Phys. B **42**, 075503 (2009).
[28] R. W. Boyd, *Nonlinear Optics* (Academic, Boston, 1992), p. 214.